



1 **Influence of the Bermuda High on interannual variability of**  
2 **summertime ozone in the Houston-Galveston-Brazoria region**

3 **Yuxuan Wang<sup>1,2</sup>, Beixi Jia<sup>2</sup>, Sing-Chun Wang<sup>1</sup>, Mark Estes<sup>3</sup>, Lu Shen<sup>4</sup>, Yuanyu Xie<sup>2</sup>**

4 <sup>1</sup>Department of Earth and Atmospheric Sciences, the University of Houston, Houston,  
5 TX, USA

6 <sup>2</sup>Ministry of Education Key Laboratory for Earth System Modeling, Center for Earth  
7 System Science, Tsinghua University, Beijing, China

8 <sup>3</sup>Texas Commission on Environmental Quality, Austin, TX, USA

9 <sup>4</sup>School of Engineering and Applied Sciences, Harvard University, Cambridge, MA,  
10 USA

11

12 **ABSTRACT**

13 The Bermuda High (BH) quasi-permanent pressure system is the key large-scale  
14 circulation pattern influencing summertime weather over the eastern and southern  
15 US. Here we developed a multiple linear regression (MLR) model to characterize the  
16 effect of the BH on year-to-year changes of monthly-mean maximum daily 8-hour  
17 average (MDA8) ozone in the Houston-Galveston-Brazoria (HGB) metropolitan  
18 region during June, July and August (JJA). The BH indicators include the longitude of  
19 the BH western edge (BH-Lon), and the BH intensity index (BHI) defined as the  
20 pressure gradient along its western edge. Both BH-Lon and BHI are selected by MLR  
21 as significant predictors ( $p < 0.05$ ) of the interannual (1990-2015) variability of the  
22 HGB-mean ozone throughout JJA, while local-scale meridional wind speed is selected  
23 as an additional predictor for August only. Local-scale temperature and zonal wind



24 speed are not identified as important factors for any summer month. The best-fit  
25 MLR model can explain 61%-72% of the interannual variability of the HGB-mean  
26 summertime ozone over 1990-2015 and shows good performance in cross-validation  
27 ( $R^2$  higher than 0.48). The BH-Lon is the most important factor, which alone explains  
28 38%-48% of such variability. The location and strength of the Bermuda High appears  
29 to control whether or not low-ozone maritime air from the Gulf of Mexico can enter  
30 southeastern Texas and affect air quality. This mechanism also applies to other  
31 coastal urban regions along the Gulf Coast (e.g. New Orleans, LA; Mobile, AL; and  
32 Pensacola, FL), suggesting that the BH circulation pattern can affect surface ozone  
33 variability through a large portion of the Gulf Coast.

34

35 **Keyword:** Bermuda High, ozone, Houston, Gulf Coast, multiple linear regression

36

## 37 1. Introduction

38 Surface ozone, as an important air pollutant, has significant adverse impacts on  
39 both public health and agriculture (NRC, 1991). Ozone is produced in the  
40 troposphere by photochemical oxidation of carbon monoxide (CO) and volatile  
41 organic carbon (VOCs), initiated by reaction with hydroxyl radicals (OH) in the  
42 presence of nitrogen oxides ( $\text{NO}_x$ ). Surface ozone is influenced not only by emissions  
43 of its precursors but also by meteorological conditions (e.g. Jacob and Winner 2009).  
44 Large-scale circulation patterns can lead to local meteorological conditions that are  
45 favorable for ozone episodes, such as high temperatures, low wind speeds, clear



46 skies, and stagnation (Nielsen-Gammon et al., 2005; Ngan and Byun, 2011; Pearce et  
47 al., 2011; Psilogloue et al., 2013; Pugliese et al., 2014). Previous studies have  
48 demonstrated certain associations between large-scale circulations and surface  
49 ozone concentrations over the US (e.g. Darby, 2005; Rappenglück et al., 2008; Lin et  
50 al., 2012; Zhu and Liang, 2013; Shen et al., 2015; Lin et al., 2015). For example,  
51 surface ozone in the western US is affected by mid-latitude cyclones that transport  
52 Asian pollutions eastward across the Pacific (Lin et al., 2012) and late-spring  
53 stratospheric intrusions occurring more frequently following strong La Nina winters  
54 (Lin et al., 2015). In the Midwest and Northeast US, polar jet frequency is a good  
55 indicator for the interannual variability of surface ozone in summer (Shen et al.,  
56 2015).

57 The Bermuda High (BH), a quasi-permanent system located over the North  
58 Atlantic Ocean (Davis et al., 1997), is the key large-scale circulation pattern that  
59 influences the regional climate over the eastern and southern US in summer (Li et al.,  
60 2012; Zhu and Liang, 2013; Hegarty et al., 2007; Hogrefe et al., 2004). The BH  
61 circulation pattern influences ozone air quality in the US through two mechanisms.  
62 First, as the BH shifts westward from late spring to summer, it places the eastern US  
63 under the high pressures, resulting in meteorological conditions favorable for local  
64 production of ozone, such as high temperatures, clear skies, and stagnation. A  
65 number of studies have shown that high ozone concentrations easily occur over  
66 large parts of the Northeast under the BH pressure pattern (Eder et al., 1993; Fiore  
67 et al., 2003; Hogrefe et al., 2004). Second, the southerly flows at the western edge of



68 the BH bring clean marine air from the Gulf of Mexico to the southern Great Plains  
69 (Higgins et al. 1997). This maritime inflow has lower concentrations of ozone  
70 compared with the continental air it replaces, thus responsible for low ozone  
71 background over much of the Gulf States in summer (Langford et al., 2009; Ngan and  
72 Byun et al., 2011). These two mechanisms have been illustrated by Zhu and Liang  
73 (2013). Using observational data, they found positive correlations over the Northeast  
74 between maximum daily 8h average (MDA8) surface ozone in summer and the  
75 intensity of the BH on the interannual time scale due to the first mechanism, but  
76 negative correlations over the South-Central US due to the second mechanism. Shen  
77 et al. (2015) further suggested that the location of the BH western edge has an  
78 influence on the summer mean MDA8 ozone in the Southeast.

79 The Houston-Galveston-Brazoria (HGB) area is a major metropolitan area on the  
80 Gulf coast located near the western edge of the BH in summer (Figure 1). The HGB  
81 region was classified as a “marginal” nonattainment zone for ozone by the U.S.  
82 Environmental Protection Agency (EPA) under the 2008 standard (TCEQ, 2012),  
83 although mean and peak ozone of the HGB area has decreased significantly during  
84 the past decades due to control of anthropogenic emissions (Berlin et al. 2013). A  
85 number of studies have demonstrated the importance of meteorology and  
86 circulation patterns on ozone over the HGB (Ngan et al., 2011; Rappenglück et al.,  
87 2008; Pakalapati et al., 2009; Haman et al., 2014), focusing predominantly on a  
88 typical year or episodic high ozone cases, such as those observed during the Texas  
89 Air Quality Study-II (Rappenglück et al., 2008; Bridget et al., 2009). Doppler lidar



90 measurements of the strength and direction of the nocturnal low level jet (LLJ)  
91 during the TexAQS 2006 field campaign (Tucker et al., 2009) found a relationship  
92 between the nocturnal LLJ and ozone concentrations on the next day. A strong  
93 southerly nocturnal LLJ was linked to the influence of the BH. Given the evidence  
94 established by prior investigations on the overall influence of the BH on summertime  
95 ozone over the southern US (e.g. Zhu and Liang 2013; Shen et al., 2015), we  
96 hypothesize that the large-scale circulation patterns associated with the BH play a  
97 key role in driving the year-to-year change in surface ozone over the HGB. In this  
98 study we will test this hypothesis by examining the statistical relationship between  
99 the variability of the BH and MDA8 ozone over the HGB during June, July, and August  
100 (JJA), a time period when the BH is located closer to North America and exerts large  
101 influences to circulation patterns over the HGB.

102

## 103 **2. Data and Methods**

### 104 **2.1. Ozone observations**

105 The HGB region is delineated by longitude from  $-94.5^{\circ}\text{W}$  to  $-96.0^{\circ}\text{W}$ , and by  
106 latitude from  $28.5^{\circ}\text{N}$  to  $30.5^{\circ}\text{N}$  (blue box in Figure 1a). Surface ozone concentrations  
107 over the HGB have been routinely monitored at continuous ambient monitoring  
108 stations (CAMSs) maintained by the Texas Commission on Environmental Quality  
109 (TCEQ), the City of Houston, and Harris County. Observational records of surface  
110 ozone in JJA from 1990 to 2015 were obtained from the EPA AirData website



111 ([http://www3.epa.gov/airquality/airdata/ad\\_data\\_daily.html](http://www3.epa.gov/airquality/airdata/ad_data_daily.html)). Ozone observations  
112 from 28 ozone CAMS sites in the HGB region that have data records longer than 10  
113 years were used for analysis. Figure 1b displays the site distributions and long-term  
114 mean ozone in JJA at each site. The site locations and operation time periods are  
115 provided in the supplementary material (Table S1). The number of CAMS sites  
116 increases to 16 in 1998 and 21 in 2004. There are 8 sites with continuous  
117 observations from 1990 to present. The overall data coverage at each selected site is  
118 99% during its operation period, except the Houston East site that has ozone  
119 observations since 1990 but no data during 1993-1995. In what follows, all the ozone  
120 data and related discussions are MDA8 ozone and the correlation coefficient,  $r$ ,  
121 reported in this study is the Pearson correlation coefficient unless stated otherwise.

122 As shown in Figure 1b, the sites in Galveston and Brazoria counties have lower  
123 ozone concentrations than the sites in the Houston region, due in part to lower local  
124 emissions. Since the scope is on synoptic scale circulation patterns, we focus on the  
125 HGB-mean ozone rather than ozone at individual sites. To calculate the HGB-mean  
126 ozone for a given month, we averaged ozone observations from all eligible sites  
127 (all-site average) and compared that with the average of only those sites with  
128 continuous observations since 1990 (continuous-site average). The difference in the  
129 HGB-mean ozone calculated from the two averaging approaches is within 5 ppbv and  
130 diminishes in the 2000s as the sites number increases (Fig 2a). To remove the  
131 influence of the decreasing trend in anthropogenic emissions on the interannual  
132 variability of ozone, the HGB-mean ozone of each month (JJA) was de-trended by



133 subtracting the 7-year moving average of the corresponding month. The de-trending  
134 process further decreases the difference in the HGB-mean ozone calculated from the  
135 two averaging approaches (Fig 2b). Therefore we use the all-site average to present  
136 the HGB-mean ozone. The time series of the de-trended HGB-mean ozone is from  
137 1993 to 2012.

## 138 **2.2. Meteorological data**

139 The meteorological data consists of the geopotential height at 850hPa and sea  
140 level pressure (SLP) from the National Centers for Environmental Prediction (NCEP)  
141 Reanalysis 1 with a spatial resolution of  $2.5^{\circ} \times 2.5^{\circ}$  (Kalnay et al., 1996), which were  
142 used to derive the BH indices described below. We adopted 2-meter temperature (T),  
143 zonal (U) and meridional (V) component of wind on 850hPa from the European  
144 Centre for Medium-Range Weather Forecasts (ECMWF) Interim reanalysis with a  
145 finer spatial resolution of  $0.5^{\circ} \times 0.5^{\circ}$ . These data were used to calculate the local-scale  
146 meteorological parameters, including the HGB-mean temperature and 850 hPa  
147 winds (U and V).

## 148 **2.3. BH indices**

149 Figure 3 illustrates the mean BH circulation patterns from June to August. The  
150 HGB region is located to the west of the BH, thus under strong southerly winds from  
151 June to August. The intensity of the BH peaks in July. As the BH intensifies from June  
152 to July, its west edge moves westward toward the North America continent; when it  
153 weakens from July to Aug, its west edge retreats eastward away from the continent.



154 Separate indices have been used to define the intensity and location of the BH  
155 (Stahle and Cleaveland, 1992; Ortegren et al. 2011, Li et al. 2011; Zhu and Liang,  
156 2013). For the BH location, we adopted the BH longitudinal index (BH-Lon) from Li et  
157 al. (2011) as a measure of the westward extension of the BH. They defined the  
158 BH-Lon as the longitude of the cross point of the 1560 geopotential meter (gpm)  
159 isoline and the 850hPa wind ridgeline. The BH-Lon is always negative in longitude,  
160 thus more negative values meaning closer proximity to the US.

161 The intra-seasonal variability of the BH (c.f. Fig 3) will affect the value of BH-Lon  
162 when defined with reference to a fixed isoline. For instance, the 1560 gpm isoline is  
163 located further away from the HGB in August when the BH is weaker than in July,  
164 even when the center location of the BH from the HGB does not change between the  
165 two months. To reduce such effect, we tried different isolines with an interval of 4  
166 gpm from 1560 to 1536 gpm in the calculation of the BH-Lon by month and  
167 evaluated which definition captures the most variability of the HGB-mean ozone. For  
168 June and July, the BH-Lon is best defined on the basis of the 1560 gpm isoline, the  
169 same as in Li et al. (2011), and this definition results in the interannual (1993-2012)  
170 correlation ( $r$ ) of 0.69 between detrended BH-Lon and HGB-mean ozone. The BH-Lon  
171 for August is defined using the 1556 gpm and the corresponding  $r$  is 0.62.

172 The time series of monthly-mean BH-Lon is shown in Figure 4. In  
173 correspondence with the intra-seasonal movement of the BH shown in Fig 3, the  
174 mean value of BH-Lon from 1990-2015 was 80.3°W in June, 93.1°W in July, and  
175 91.6°W in August. There were no significant trends in BH-Lon for the months of June





176 and July. In August, however, BH-Lon exhibited a significant increasing trend (i.e., an  
177 eastward shift) of  $0.51^\circ \text{ a}^{-1}$  ( $p < 0.1$ ) over 1990-2015. Shen et al. (2015) found an  
178 increasing trend of  $0.35^\circ \text{ a}^{-1}$  in the JJA-mean BH-Lon over 1980 - 2010 using the  
179 definition of Li et al. (2011). Rather than a change in the BH circulation patterns, they  
180 attributed this trend to a spatially uniform decrease of SLP over the US and adjacent  
181 Atlantic Ocean in the reanalysis data. Given their work as well as the lack of a  
182 consistent trend in the monthly-mean BH-Lon over 1990-2015, we do not consider  
183 the trend of BH-Lon in the present work and the BH-Lon time series were de-trended  
184 by removing the 7-year moving averages.

185 Another type of BH index is defined on the basis of pressure differences  
186 between two representative locations, with their exact locations varying among  
187 studies. Zhu and Liang (2013) defined a pressure-based BH index (BHI) as the mean  
188 SLP difference between a location in the Gulf of Mexico and the other in the  
189 southern Great Plains where the SLP has the largest positive and negative correlation  
190 with LLJ respectively. As a result, their BHI exhibits a significant positive association  
191 between the strength of LLJ, which determines the transport of clean marine air  
192 from the Gulf of Mexico. Similar to that study, we defined a pressure-based BHI as  
193 the mean SLP difference along the west edge of the BH, between the same location  
194 in the Gulf of Mexico as selected by Zhu and Liang (2013) ( $25.3^\circ$ - $29.3^\circ\text{N}$ ,  
195  $92.5^\circ$ - $87.5^\circ\text{W}$ ) (box 1 in Figure 1a) and the other in southern Great Plains ( $35^\circ$ - $39^\circ\text{N}$ ,  
196  $105.5^\circ$ - $100^\circ\text{W}$ ) (box 2 in Figure 1a) where the SLP exhibits the largest correlation  
197 with the HGB-mean ozone. This BHI shows only weak to moderate correlations with



198 BH-Lon, with  $r$  being -0.57, -0.26 and -0.39 for JJA respectively, suggesting the  
199 position of the BH west edge may not vary coherently with the pressure gradient  
200 over the west edge. Therefore, both BH-Lon and BHI are used as predictors in the  
201 regression model described below.

## 202 **2.4. Statistical Method**

203 We applied a multiple linear regression (MLR) model, which has been  
204 commonly used in air quality and meteorological studies (e.g. Kutner et al., 2004; Tai  
205 et al., 2010), to construct the statistical relationship between the detrended  
206 HGB-mean ozone and the five meteorological predictors described above, including  
207 BH-Lon, BHI, T, U, and V. Since our focus is on variability, all the meteorological  
208 predictors were detrended using the same approach as the ozone data. For ease of  
209 comparison, all the meteorological predictors in the regression analysis were  
210 normalized. The regression was conducted on the monthly scale from 1993 to 2012.  
211 The model is of the form:

$$212 \quad y = \beta_0 + \sum_{k=1}^n \beta_k x_k \quad (1)$$

213 where  $y$  is the detrended monthly HGB-mean MDA8  $O_3$ ,  $n$  is the number of  
214 predictors,  $x_k$  represents the  $k^{\text{th}}$  predictor which is detrended and normalized,  $\beta_k$   
215 is the corresponding regression coefficient for  $x_k$ , and  $\beta_0$  is the intercept. The  
216 predictors are separated into two groups. We applied a stepwise regression using  
217 the BH indices (BH-Lon, BHI) first, which represent the large-scale effects. The  
218 HGB-mean T, U, and V that characterize local meteorological conditions were added



219 subsequently only if they result in significant improvements in model performance.  
220 The predictor selection is based on the Akaike Information Criterion (AIC) statistics to  
221 obtain the best model fit (Venables and Ripley, 2003).

222

### 223 **3. RESULTS**

#### 224 **3.1. Ozone and the BH relationship**

225 The HGB-mean ozone shows a large intra-seasonal variation during JJA (Figure  
226 5), with a minimum of monthly-mean ozone in July. We first examined if this feature  
227 can be explained by near-surface temperature, which has been suggested as an  
228 important meteorological factor affecting surface ozone in many regions (Fu et al.,  
229 2015; Rasmussen et al., 2012; Camalier et al., 2007). As shown in Figure 5, the  
230 HGB-mean temperature is the highest in July when the monthly mean ozone is  
231 lowest, precluding temperature as the driver of the intra-summer variability of  
232 ozone over the HGB region. This can be explained by the fact that summertime  
233 temperatures over the HGB region are always high, thus the temperature variation is  
234 relatively less significant and the ozone formation might not be limited by  
235 temperature over this region in summer. To further support this argument, on the  
236 interannual time scale (1993-2012) the HGB-mean ozone shows no correlation with  
237 temperature in June ( $r = -0.14$ ), although the correlation coefficient between the two  
238 increases to 0.29 and 0.41 in July and August, respectively.

239 The BH-Lon reaches its westernmost location in July (Figure 3), coincident with



240 the ozone minimum (monthly mean) in the same month. This coincidence supports  
241 the mechanism that the more westward shift of the BH (the lower BH-Lon) brings  
242 the stronger inflow of cleaner maritime air into the HGB leading to lower surface  
243 ozone. The decrease of background ozone over the HGB region from spring to  
244 summer is reported by a number of observational and modeling studies  
245 (Nielsen-Gammon et al., 2005a; Nielsen-Gammon et al., 2005b; Li et al., 2002;  
246 Reidmiller et al., 2009) and can be attributed to strengthening of this maritime  
247 inflow in summer. Indeed, as shown in Figure 6a, the BH-Lon shows a significantly  
248 stronger correlation with the HGB-mean ozone during JJA ( $r = 0.62\sim 0.69$ ) than  
249 temperature does. However, the BH-Lon does not correlate well with the HGB-mean  
250 temperature, with  $r$  being -0.04, 0.44, and 0.33 for JJA respectively. The BH-Lon has a  
251 higher correlation with the HGB-mean meridional wind ( $V$ ) ( $r = -0.4\sim -0.7$ ) but does  
252 not correlate with the zonal wind ( $U$ ). This is expected because the BH determines  
253 the strength of the meridional flows that bring maritime air masses from the Gulf of  
254 Mexico to southeastern Texas.

255 Given the intra-summer variations described above, the effects of the BH on the  
256 HGB-mean ozone are analyzed month by month in the following sections. For  
257 comparison, Zhu and Liang (2013) combined the intra-seasonal and interannual  
258 variations of ozone and Shen et al. (2015) focused on the variability of the JJA-mean  
259 ozone. Both studies investigated the southern US as a whole.

### 260 **3.2. Statistical model**

261 Using the stepwise regression (Equation 1), we obtained the best-fit MLR



262 equations for the interannual variability of the HGB-mean ozone by month. Table 1  
263 summarizes the regression results, including the predictors selected for each month  
264 and their regression coefficients. Both BH-Lon and BHI are selected as significant  
265 predictors ( $p < 0.05$ ) for each month, while V is selected as an additional predictor  
266 for August only. Temperature is not selected as a predictor by the MLR for any  
267 month, which is consistent with insignificant correlation between ozone and  
268 temperature presented above. The HGB-mean zonal wind (U) is not selected for any  
269 month either. The squares of the Pearson correlation coefficients ( $R^2$ ) from the MLR  
270 are 0.61 for Jun, 0.72 for Jul, and 0.70 for Aug.

271 Figure 7 displays the time series of the observed and MLR-regressed  
272 monthly-mean ozone (both detrended) from 1993 to 2012. Many of the extremely  
273 high and low ozone months are well reproduced by the MLR model, for example, the  
274 low ozone month of June 2004 and high ozone month of August 2011. The BH-Lon is  
275 the most important predictor throughout JJA and has the highest regression  
276 coefficient (absolute values) that is positive throughout JJA (Table 1). Given the  
277 BH-Lon being negative, this means that as the Bermuda High extends more  
278 westward, ozone over the HGB is lowered, which supports the mechanism that the  
279 BH brings maritime inflow of low ozone background into the HGB region. The MLR  
280 relationship indicates that monthly-mean MDA8 ozone over the HGB area will  
281 decrease by 4.52, 3.44, and 3.34 ppbv, respectively, for every degree of westward  
282 extension of the BH-Lon in June, July, and August.

283 While the MLR model developed here captures 61%-72% (based on  $R^2$ ) of the



284 interannual variance of the HGB-mean ozone from June to August, the  
285 meteorological predictors may be correlated with each other, leading to overfitting  
286 of the data. To examine the multi-collinearity between the meteorological predictors,  
287 the variance inflation factor (VIF), a widely used index of the collinearity in the  
288 regression analysis, was calculated for each variable. Table 2 summarizes the VIF of  
289 each predictor by month. Most of the VIF is smaller than 3, much lower than the  
290 commonly-used VIF threshold of 10 in determining significant collinearity (Kutner et  
291 al., 2004), indicating the problem of multi-collinearity among the predictors is  
292 generally unimportant.

### 293 **3.3. Model cross-validation**

294 The MLR model described above shows good regression performance in  
295 explaining the interannual variations of the summertime HGB-mean ozone on the  
296 monthly scale. To evaluate the predictability of this model, a cross-validation (CV)  
297 method was implemented. We first isolated one year at a time, performed model  
298 fitting with the remaining years, and then applied the model to predict the  
299 monthly-mean ozone on the isolated year. Figure S1 shows the CV results by month.  
300 The  $R^2$  between the observed and CV-predicted ozone is 0.48~0.59, indicating the  
301 MLR model is capable of predicting about 50% interannual (1993-2012) variability of  
302 monthly mean ozone over the HGB area in summer. However, some of the extreme  
303 ozone values are not well predicted, suggesting that other factors are responsible for  
304 those high ozone events, e.g. emissions and stagnation conditions, which are not  
305 considered as predictors in the MLR model.



306

## 307 **4. DISCUSSION**

### 308 **4.1. Comparison with other studies**

309 To the best of our knowledge, the MLR-regression correlation coefficients ( $r =$   
310  $0.78 \sim 0.84$ ) are significantly higher than those from previously published studies on  
311 the regression relationship between interannual variability of meteorological factors  
312 and surface ozone over a metropolitan region or the southern US as a whole. Zhu  
313 and Liang (2013) reported a negative correlation of  $-0.5 \sim -0.7$  between the BHI and  
314 summer-mean MDA8 ozone during 1993-2010. Shen et al. (2015) identified the polar  
315 jet, the Great Plains low level jet, and the BH as major synoptic-scale patterns  
316 influencing surface  $O_3$  variability in the eastern US in summer, which in combination  
317 explain 53% ( $r = 0.73$ ) of the interannual variance of summer-mean MDA8 ozone in  
318 South Central US during 1980-2010. These studies averaged surface ozone over a  
319 large geographical region and onto a seasonal mean and thus smoothed out some  
320 variability. By comparison, the present study investigates the interannual variability  
321 of monthly mean ozone over a smaller region (HGB) and extends to more recent  
322 time periods (1990-2015). With just three meteorological predictors (BH-Lon, BHI,  
323 and V), the MLR model developed here captures 61% - 72% of the interannual  
324 variance of the HGB-mean ozone during JJA. The MLR model developed here shows  
325 a good prediction skill with the CV  $R^2$  higher than 0.48 for each month of JJA.

### 326 **4.2. Mechanism**



327           Among the meteorological predictors examined here, indicators of the BH  
328   location (BH-Lon) and strength (BHI) explain more interannual variability of the  
329   summertime HGB-mean ozone than local meteorological factors (i.e. winds and  
330   temperature), indicating the dominant role of large-scale circulation patterns  
331   controlling ozone variability over this region in summer. The BH-Lon is the most  
332   important predictor throughout JJA, which alone explains 38%-48% of the observed  
333   interannual variability of monthly mean ozone over the HGB region. As discussed  
334   above, the BH circulation patterns in summer are responsible for the inflow of low  
335   ozone air masses from the Gulf of Mexico into the HGB region. The MLR results  
336   suggest that the BH-Lon is a better predictor than local-scale meridional wind to  
337   indicate the variability of this maritime inflow and consequently surface ozone.

338           As a further illustration of this mechanism, Figure 8 compares circulation  
339   patterns and associated changes in the HGB-mean ozone between two  
340   representative months, Jul 2000 and Jul 2001. The BH was not only stronger in Jul  
341   2001 but also extended closer to the southeastern US during that month than Jul  
342   2000. The BH-Lon was 88.7°W in Jul 2001 as compared to that of 78.7°W in Jul 2000,  
343   indicating stronger maritime influence to HGB during the former month.  
344   Correspondingly, surface ozone concentrations were significantly lower at all the  
345   CAMs monitors during Jul 2001 than Jul 2000 (Fig 8). The HGB-mean ozone was 38.9  
346   ppbv in Jul 2001, compared with 49.0 ppbv in Jul 2000. The number of ozone  
347   nonattainment days was also lower in Jul 2001 (2 days) than Jul 2000 (6 days).  
348   Despite different BH-Lon, the HGB-mean V happened to be the same during the two





349 months, both -2.1 m/s. This indicates that local-scale wind alone may not be  
350 sufficient to indicate the origin of air masses because winds are affected by both  
351 large-scale and local-scale factors.

352         Given the large-scale influence of the BH, the mechanism underlying the BH and  
353 O<sub>3</sub> association over the HGB region, if correct, should apply for other urban regions  
354 along the Gulf Coast which experience similar onshore maritime flow from the Gulf  
355 of the Mexico in summer. To test this, we chose New Orleans in Louisiana  
356 (29.8°-30.6°N, 89.9°-90.7°W), Mobile in Alabama (30.4°-30.8°N, 88.0°-88.2°W), and  
357 Pensacola in Florida (30.3°-30.5°N, 87.2°-87.3°W), all of which are at about 30°  
358 latitude, similar to HGB. Figure 6b-d presents the time series of surface ozone  
359 (detrended and averaged over all the CAMS monitors) at these urban areas during  
360 JJA along with BH-Lon. On interannual time scales (1993-2013), monthly mean ozone  
361 concentrations at the three urban regions all exhibit significantly positive  
362 correlations with the BH-Lon throughout JJA ( $r = 0.38\sim 0.64$ ), which is consistent with  
363 the BH-O<sub>3</sub> association over HGB and thus confirms the large-scale impact of the BH  
364 circulation patterns on surface ozone variability along the Gulf Coast. It is interesting  
365 to note that the BH-O<sub>3</sub> correlation coefficients at HGB are highest among the four  
366 urban regions along the Gulf Coast. This can be partly explained by the fact that HGB  
367 has the largest quantity of ozone-precursor emissions among the four urban areas,  
368 so that the intrusion of clean maritime air masses would cause a larger relative  
369 reduction of ozone at HGB, and therefore the BH location and strength could cause  
370 more ozone variability.



371 **4.3. Threshold value of BH-Lon**

372 Shen et al. (2015) identified a threshold value of 85.4°W for the JJA-mean  
373 BH-Lon that marks two different associations of the BH-Lon with surface ozone in the  
374 eastern US. When the BH-Lon is east of 85.4°W, westward movement of the BH-Lon  
375 leads to a decrease of surface ozone; when it is west of that threshold, its westward  
376 movement leads to an increase of ozone. We did not find such a threshold value of  
377 BH-Lon for the monthly scale analysis presented above; the monthly-mean  
378 relationship between BH-Lon and HGB-mean ozone is consistently linear throughout  
379 the study period for each summer month (c.f. Fig 6 and Fig S1).

380 On the daily scale, however, we found evidence for a threshold of BH-Lon that  
381 tends to create conducive or non-conductive conditions for high ozone days over the  
382 HGB region. Figure 9a shows the variation of HGB-mean daily ozone anomaly as a  
383 function of daily BH-Lon during July 2011, a high ozone month. The daily ozone  
384 anomaly is calculated as the difference between daily and 30-day moving average of  
385 ozone. The daily data shown in Fig 9a clearly display two populations, warranting a  
386 threshold of BH-Lon to separate them. As a simplified attempt, a linear piecewise  
387 fitting was applied to the daily data, using different segmentation points with varying  
388 BH-Lon from 100° W to 80° W at an interval of 0.5°. The least regression error (sum  
389 of the squared errors) was obtained when the segmentation point was set to 90° W,  
390 which represents the threshold of BH-Lon for July 2011. The resulting regression  
391 indicates that when the BH-Lon is east of 90°W, the westward extension of BH-Lon  
392 tends to cause a decrease of HGB ozone; the opposite relationship holds when the



393 BH-Lon is west of that threshold (Fig 9).

394 To understand causes of the two regimes, Figure 9b-c compares circulation  
395 patterns between two representative days, July 3 and July 10 2011, when the BH-Lon  
396 is located to the west and east of its threshold respectively. The circulation patterns  
397 on July 10 (9c), when the BH-Lon was located to the east of 90°W, are similar to the  
398 typical monthly-mean patterns described before: clean maritime air masses flow  
399 southeasterly to southeast Texas along the west edge of the BH, leading to lower  
400 surface ozone in HGB (26.4 ppbv on July 10 2011). On July 3 (9b), there was a  
401 high-pressure system over southeast US, which appears to be separate from the BH  
402 and in this case the choice of 1560 gpm isoline may not be appropriate to define the  
403 BH west edge on a daily scale. According to the wind fields, however, this  
404 high-pressure system over land is likely resulted from the westward extension of the  
405 BH to the continental US. The high-pressure system typically brings stagnant weather,  
406 high temperatures, and clear skies, which are all favorable meteorological conditions  
407 leading to higher ozone on July 3 (42.2 ppbv).

408 To predict daily ozone on the basis of its statistical relationships with  
409 meteorology alone is a challenging task and beyond the scope of the present study.  
410 The simple daily analysis presented above for the month of July 2011 was intended  
411 to demonstrate that the linear relationship between the BH-Lon and HGB-mean  
412 ozone on a monthly scale is useful to explain some portion of HGB ozone variability  
413 on a daily scale, but there are certain degrees of nonlinearity in the daily relationship  
414 associated with a threshold value of the BH-Lon that separates different circulation



415 regimes and that threshold value may not be constant for every month. When the  
416 BH-Lon is used to predict the monthly-mean ozone over the HGB area, however, it is  
417 not necessary to consider the threshold of BH-Lon since the mean variations of the  
418 BH-Lon is a lot smaller on the monthly scale than that on the daily time scale.

419

## 420 **5. Conclusion**

421 More than two decades (1990 - 2015) long observational record of MDA8 ozone  
422 and meteorology were analyzed to characterize the effects of the BH circulation  
423 patterns on interannual variations of surface ozone in the HGB region during the  
424 summer months (June to August). The BH indicators are the longitude of the BH  
425 western edge (BH-Lon) and the pressure-based BH intensity index (BHI) along its  
426 western edge. Statistical relationships between the HGB-mean ozone variability and  
427 meteorological predictors, including both large-scale (BH-Lon, BHI) and local-scale  
428 ones (T, U, V), were tested and developed through multiple linear regression (MLR).  
429 The best-fit MLR equations select both BH-Lon and BHI as significant predictors ( $p <$   
430  $0.05$ ) of interannual variability of the HGB-mean ozone for each month and  
431 meridional wind speed (V) as a significant predictor for August only. Temperature or  
432 zonal wind speed (U) is not selected as a predictor by the MLR for any of the summer  
433 month. The exclusion of temperature in the MLR model is supported by the lack of  
434 significant correlations between ozone and temperature over the HGB region on  
435 both intra-seasonal and interannual time scales. This suggests temperature is not a  
436 key driver of summertime ozone variability in the HGB region despite its importance



437 for other regions.

438 With only three meteorological predictors (BH-Lon, BHI, and V), the MLR model  
439 developed here captures 61%-72% (based on  $R^2$ ) of the interannual variance of the  
440 HGB-mean ozone from June to August. The MLR model developed here also show a  
441 good prediction skill with the CV  $R^2$  higher than 0.45. The BH-Lon alone explains  
442 38%-48% ( $r = 0.62 \sim 0.69$ ) of the year-to-year variability in monthly mean ozone over  
443 HGB during JJA for the period 1990-2015, indicating the dominant role of large-scale  
444 circulation patterns controlling ozone variability over this region in summer. Such a  
445 high correlation is explained by the mechanism that the western extension of the BH  
446 determines the strength of the inflow of maritime air masses with lower ozone  
447 background from the Gulf of Mexico to the HGB during summer. This mechanism  
448 also applies to other coastal urban regions, such as New Orleans LA, Mobile AL and  
449 Pensacola FL, confirming the large-scale impact of the BH circulation patterns on  
450 surface ozone variability along the Gulf Coast. The linear relationship between the  
451 BH-Lon and HGB-mean ozone on a monthly scale is useful to explain some portion of  
452 HGB ozone variability on a daily scale, but there are certain degrees of nonlinearity  
453 in the daily relationship associated with a threshold value of the BH-Lon that  
454 separates different circulation regimes and that threshold value may not be constant  
455 for every month. The statistical relationship between surface ozone and large-scale  
456 circulation patterns on derived herein will be useful to distinguish the role of  
457 meteorology versus anthropogenic emissions in controlling the interannual  
458 variability of ozone along the Gulf Coast as well as to serve a benchmark to test the



459 performance of air quality models in representing such distinctions, which will be  
460 investigated in future studies.

461

#### 462 **Acknowledgement**

463 This research was supported by Texas Commission on Environmental Quality  
464 (TCEQ) (Grant No. 582-13-34576) and Texas Air Quality Program (Project 14-010). B.  
465 Jia acknowledges additional funding from the National Key Basic Research Program  
466 of China (2013CB956603).

467

#### 468 **REFERENCES**

469 Berlin, S.R., A.O. Langford, M. Estes, M. Dong, D.D. Parrish: Magnitude, decadal  
470 changes, and impact of regional background ozone transported into the greater  
471 Houston, Texas area, *Environ. Sci. Technol.*, 47(24), 13985-13992, 2013.

472 Berman, J. D., N. Fann, J. W. Hollingsworth, K. E. Pinkerton, W. N. Rom, A.M. Szema,  
473 P. N. Breyse, R. H. White, F. C. Curriero: Health benefits from large-scale ozone  
474 reduction in the United States, *Environ. Health Perspect.*, 120(10), 1404-1410,  
475 2012.

476 Bridget M. Day et al., Nocturnal boundary layer characteristics and land breeze  
477 development in Houston, Texas during TexAQS II, *Atmospheric Environment*,  
478 doi:10.1016/j.atmosenv.2009.01.031, 2009.

479 Camalier, L., William Cox, Pat Dolwick: The effects of meteorology on ozone in urban  
480 areas and their use in assessing ozone trends, *Atmos. Environ.*, 41(33),



- 481           7127-7137, 2007.
- 482   Davis, R. E., B. P. Hayden , D. A. Gay , W. L. Phillips, G. V. Jones: The North Atlantic
- 483           subtropical anticyclone, *J. Climate*, 10, 728-744, 1997.
- 484   Darby, L.S.: Cluster Analysis of Surface Winds in Houston, Texas, and the Impact of
- 485           Wind Patterns on Ozone. *J. Appl. Meteor.*, 44, 1788–1806, 2005.
- 486   Eder, B. K., J. M. Davis, and P. Bloomfield, A characterization of the spatiotemporal
- 487           variability of non-urban ozone concentrations over the eastern United States,
- 488           *Atmos. Environ.*, 27A(16), 2645–2668, 1993
- 489   Fiore, A.M., D.J. Jacob, I. Bey, R.M. Yantosca, B.D. Field, A.C. Fusco: Background
- 490           ozone over the United States in summer: origin, trend, and contribution to
- 491           pollution episodes, *J. Geophys. Res.*, 107 (D15), 2002.
- 492   Fiore, A.M., D.J. Jacob, R. Mathur, R.V. Martin, Application of empirical orthogonal
- 493           functions to evaluate ozone simulations for the eastern United States with
- 494           regional and global models, *J. Geophys. Res.*, 108, 4431,
- 495           doi:10.1029/2002JD003151, 2003
- 496   Haman, C. L., E. Couzo, J. H. Flynn, W. Vizuete, B. Heffron, and B. L. Lefer:
- 497           Relationship between boundary layer heights and growth rates with
- 498           ground-level ozone in Houston, Texas, *J. Geophys. Res.*, 119 (10), 6230-6245,
- 499           2014.
- 500   Hegarty, J., H. Mao, R. Talbot: Synoptic controls on summertime surface ozone in the
- 501           northeastern United States, *J. Geophys. Res.*, 112, D14306, 2007.
- 502   Higgins, R. W., Y. Yao, E. S. Yarosh, J. E. Janowiak, K. C. Mo: Influence of the Great



- 503 Plains low-level jet on summertime precipitation and moisture transport over  
504 the central United States, *J. Climate*, 10, 481-507, 1997.
- 505 Hogrefe, C., J. Biswas, B. Lynn, K. Civerolo, J. Y. Ku, J. Rosenthal, C. Rosenzweig, R.  
506 Goldberg, P. L. Kinney: Simulating regional-scale ozone climatology over the  
507 eastern United States: model evaluation results, *Atmos. Environ.*, 38, 2627-2638,  
508 2004.
- 509 Jacob, D. J., and Winner, D. A.: Effect of climate change on air quality, *Atmos.*  
510 *Environ.*, 43(1), 51-63, 2009.
- 511 Kalnay, E., et al.: The NMC/NCAR CDAS/Reanalysis Project, *Bull. Am. Meteorol.*  
512 *Soc.*, 77, 437-471, 1996.
- 513 Kutner, M. H., C. J. Nachtsheim, J. Neter, W. Li: *Applied Linear Statistical Models*.  
514 McGraw-Hill/Irwin, New York, NY, USA, 2004.
- 515 Langford, A. O., C. J. Senff, R. M. Banta, R. M. Hardesty, R. J. Alvarez II, S. P. Sandberg,  
516 and L. S. Darby, Regional and local background ozone in Houston during Texas  
517 Air Quality Study 2006, *J. Geophys. Res.*, 114, D00F12, 2009.
- 518 Li, W., L. Li, R. Fu, Y. Deng, and H. Wang: Changes to the North Atlantic subtropical  
519 high and its role in the intensification of summer rainfall variability in the  
520 southeastern United States, *J. Climate*, 24, 1499-1506, 2011.
- 521 Li, L., W. Li, Y. Kushnir: Variation of North Atlantic Subtropical High western ridge and  
522 its implication to the Southeastern US summer precipitation, *Clim. Dyn.*,  
523 39:1401-1412, 2012.
- 524 Li, Q., D. J. Jacob, T. D. Fairlie, H. Liu, R. M. Yantosca, and R. V. Martin: Stratospheric





- 525           versus pollution influences on ozone at Bermuda: Reconciling past analyses, J.  
526           Geophys. Res., 107, 2002.
- 527   Lin, M., A. M. Fiore, L. W. Horowitz, O. R. Cooper, V. Naik, J. Holloway, B. J. Johnson,  
528           A. M. Middlebrook, S. J. Oltmans, I. B. Pollack, T. B. Ryerson, J. X. Warner, C.  
529           Wiedinmyer, J. Wilson, B. Wyman: Transport of Asian ozone pollution into  
530           surface air over the western United States in spring, J. Geophys. Res., 117, 2012.
- 531   Lin, M., A. M. Fiore, L. W. Horowitz, A. O. Langford, S. J. Oltmans, D. Tarasick, H. E.  
532           Rieder: Climate variability modulates western US ozone air quality in spring via  
533           deep stratospheric intrusions, Nature Communications, 2015.
- 534   McDonald-Buller, E. C., D. T. Allen, N. Brown, D. J. Jacob, D. Jaffe, C. E. Kolb, A. S.  
535           Lefohn, S. Oltmans, D. D. Parrish, G. Yarwood, L. Zhang : Establishing Policy  
536           Relevant Background (PRB) Ozone Concentrations in the United States, Environ.  
537           Sci. Technol., 45, 9484- 9497, 2011.
- 538   Nielsen-Gammon, J. Tobin, A. McNeel, and G. Li: A conceptual model for eight-hour  
539           ozone exceedances in Houston, Texas, Part I: Background ozone levels in  
540           eastern Texas, Houston Adv. Res. Cent., Houston, Tex, 2005a.
- 541   Nielsen-Gammon, et al., A Conceptual Model for Eight-Hour Ozone Exceedances in  
542           Houston, Texas Part II: Eight-Hour Ozone Exceedances in the Houston-Galveston  
543           Metropolitan Area, Houston Adv. Res. Cent., Houston, Tex. Houston, Tex,  
544           2005b.
- 545   Ngan, F., D. Byun: Classification of Weather Patterns and Associated Trajectories of  
546           High-Ozone Episodes in the Houston-Galveston-Brazoria Area during the



- 547 2005/06 TexAQS-II, J. Appl. Meteor. Climatol., 50,485-499, 2011.
- 548 Ortegren, J. T., P. A. Knapp, J. T. Maxwell, W. P. Tyminski, and P. T. Soule: Ocean–  
549 atmosphere influences on low frequency warm-season drought variability in the  
550 Gulf Coast and southeastern United States, J. Appl. Meteor. Climatol., 50,  
551 1177-1186, 2011.
- 552 Pearce J.L, Jason Beringer, Neville Nicholls, Rob J. Hyndman, Nigel J. Tapper:  
553 Quantifying the influence of local meteorology on air quality using generalized  
554 additive models, Atmospheric Environment, 45(6):1328-1336, 2011.
- 555 Pugliese, S. C., Murphy, J. G., Geddes, J. A., and Wang, J. M.: The impacts of  
556 precursor reduction and meteorology on ground-level ozone in the Greater  
557 Toronto Area, Atmos. Chem. Phys., 14, 8197-8207, 2014.
- 558 Psiloglou, B., Larissi, I., Petrakis, M., Paliatsos, A., Antoniou, A., and Viras, L.: Case  
559 Studies on Summertime Measurements of O<sub>3</sub>, NO<sub>2</sub>, and SO<sub>2</sub> with a DOAS  
560 System in an Urban Semi-Industrial Region in Athens, Greece, Environ. Monit.  
561 Assess., 185, 7763–7774, 2013.
- 562 Rappenglück, B., R. Perna, S. Zhong, and G. A. Morris: An analysis of the vertical  
563 structure of the atmosphere and the upper-level meteorology and their impact  
564 on surface ozone levels in Houston, Texas, J. Geophys. Res., 113, D17315, 2008.
- 565 Rasmussen, D.J., A.M. Fiore, V. Naik, L.W. Horowitz, S.J. McGinnis, M.G. Schultz:  
566 Surface ozone-temperature relationships in the eastern US: A monthly  
567 climatology for evaluating chemistry-climate models Atmospheric Environment  
568 47,142-153, 2012.



- 569 Reidmiller, D. R., A. M. Fiore, D.A. Jaffe, D. Bergmann, C. Cuvelier, F.J. Dentener, et  
570 al.: The influence of foreign vs. North American emissions on surface ozone in  
571 the US, Atmos. Chem. Phys., 9, 5027-5042, 2009.
- 572 Shen, L., L. J. Mickley, A. P. K. Tai: Influence of Synoptic Patterns on Surface Ozone  
573 Variability over the Eastern United States from 1980 to 2012, Atmos. Chem.  
574 Phys., 15, 13073-13108, 2015.
- 575 Pakalapati, S., S. Beaver , J. A. Romagnoli , A. Palazoglu: Sequencing diurnal air flow  
576 patterns for ozone exposure assessment around Houston, Texas, Atmos.  
577 Environ., 43, 715-723, 2009.
- 578 Stahle, D. W., M. K. Cleaveland: Reconstruction and analysis of spring rainfall over  
579 the southeastern U.S. for the past 1000 years, Bull. Amer. Meteor. Soc., 73,  
580 1947-1961, 1992.
- 581 Tai, A.P.K., L.J. Mickley, D.J. Jacob: Correlations between fine particulate matter  
582 (PM<sub>2.5</sub>) and meteorological variables in the United States: Implications for the  
583 sensitivity of PM<sub>2.5</sub> to climate change, Atmos. Environ., 44, 3976-3984, 2010.
- 584 Tucker, S. C., R. M. Banta, A. O. Langford, C. J. Senff, W. A. Brewer, E. J. Williams, B.  
585 M. Lerner, H. Osthoff, and R. M. Hardesty (2010), Relationships of coastal  
586 nocturnal boundary layer winds and turbulence to Houston ozone  
587 concentrations during TexAQS 2006, J. Geophys. Res., 115, D10304,  
588 doi:10.1029/2009JD013169. Venables, W.N., B.D. Ripley: Modern Applied  
589 Statistics with S. Springer, New York, NY, USA, 2003.
- 590 Wang, X., D. L. Mauzerall: Characterizing distributions of surface ozone and its



591 impact on grain production in China, Japan and South Korea: 1990 and 2020,  
592 Atmos. Environ., 38, 4383- 4402, 2004.

593 Zhang, L., D.J. Jacob, N.V. Smith-Downey, D.A. Wood, D. Blewitt, C.C. Carouge, A. van  
594 Donkelaar, D.B.A. Jones, L.T. Murray, Y. Wang: Improved estimate of the  
595 policy-relevant background ozone in the United States using the GEOS-Chem  
596 global model with  $1/2^{\circ} \times 2/3^{\circ}$  horizontal resolution over North America, Atmos.  
597 Environ., 45(37), 6769-6776, 2011.

598 Zhu, J., X. Liang: Impacts of the Bermuda High on Regional Climate and Ozone over  
599 the United States, J. Climate, 26, 1018-1032, 2013.

600



601 **Tables**

602 Table 1. Regression coefficients and coefficients of determination ( $R^2$ ) of the best-fit  
603 MLR models for June, July, and August. The model cross-validation  $R^2$  is shown in  
604 the last column.

	$\beta_0$ (intercept)	BH-Lon	BHI	V	$R^2$	Adjusted $R^2$	Cross-validation $R^2$
June	0.16	4.52	-3.84	-	0.61	0.56	0.48
July	-0.26	3.44	-2.98	-	0.72	0.69	0.59
August	-0.14	3.34	3.21	-5.21	0.70	0.64	0.51

605

606

607 Table 2. Variance inflation factor (VIF) of the predictors selected in the MLR mode for  
608 June, July and August.

	BH-Lon	BHI	V
June	1.47	1.47	-
July	1.07	1.07	-
August	1.21	2.21	2.22

609

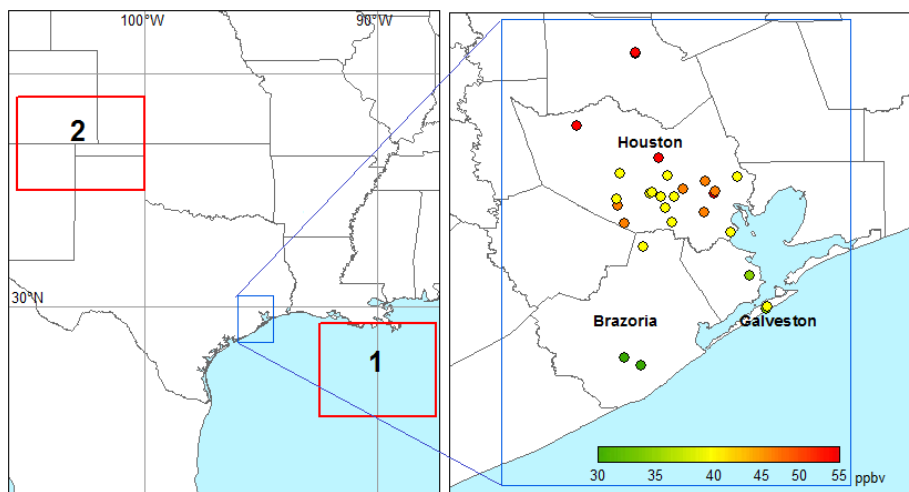
610

611



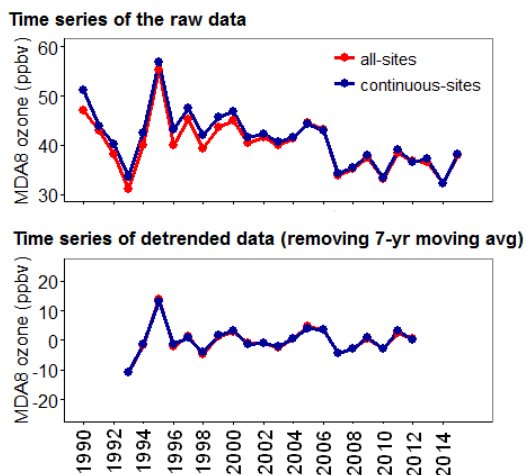
612

## Figures



613

614 Figure 1. (a) Locations of the HGB region (blue box). The red boxes show the regions  
615 used to define the BH intensity indices BHI; (b) Locations of the CAMS sites within  
616 the HGB region and the long-term (1990-2015) mean MDA8 ozone from June to  
617 August.

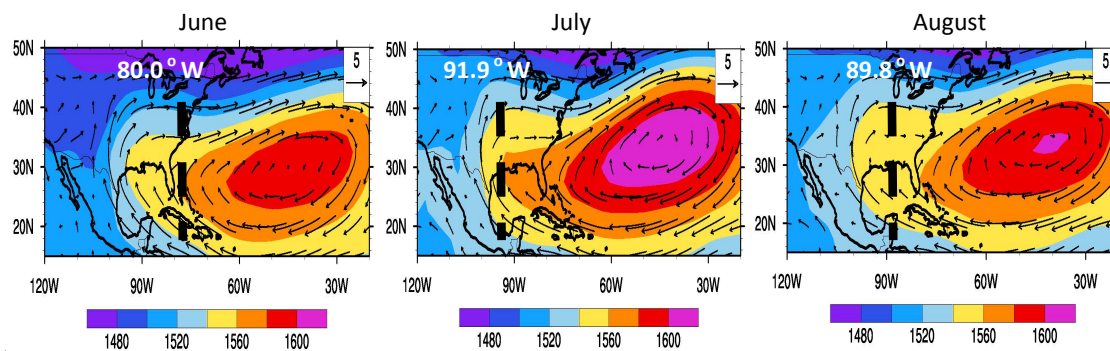


618

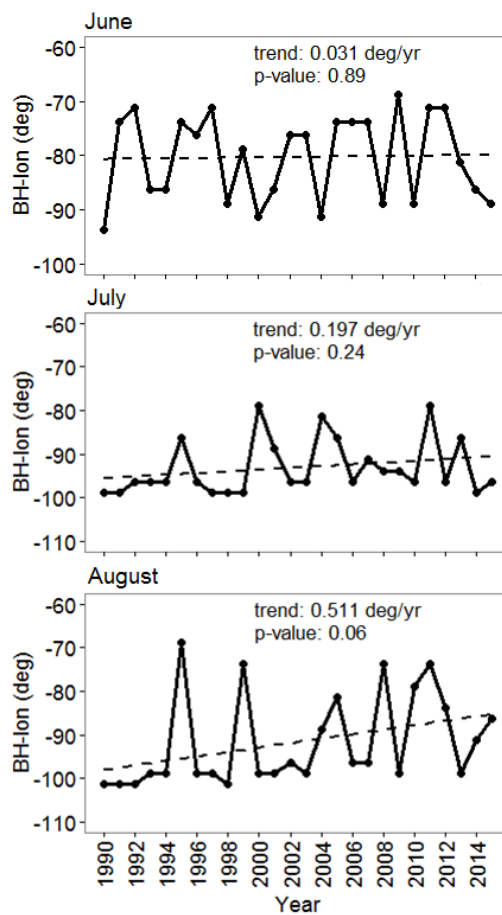
619 Figure 2. Summer (JJA)-mean ozone over the HGB area during the period from 1990  
620 to 2015. The upper panel is the time series of the raw data and the lower panel is the



621 detrended time series after subtracting the 7-year moving averages. The red line is  
622 the average from all available sites for each year and the blue line is the average of  
623 those sites with continuous coverage from 1990 to 2015.



625 Figure 3. Distributions of the 1998-2013 mean 850hPa geopotential height (color  
626 contour) and wind fields (arrows) in June (left), July (center), and August (right). The  
627 black dashed line shows the longitude of the BH-Lon (values shown in white).



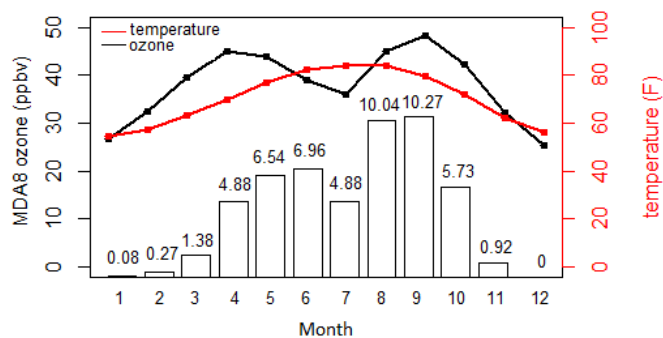
628

629 Figure 4. Time series of the BH-Lon (solid line) in June, July and August from 1990 to

630 2015. A linear trend (dash line) is used to fit each time series.

631





632

633 Figure 5. The 1990-2015 mean monthly MDA8 ozone over the HGB area (black line),

634 overlaid with the average number of exceedance days by month (bars) and the

635 HGB-mean temperature (red line). An exceedance day is defined when MDA8 ozone

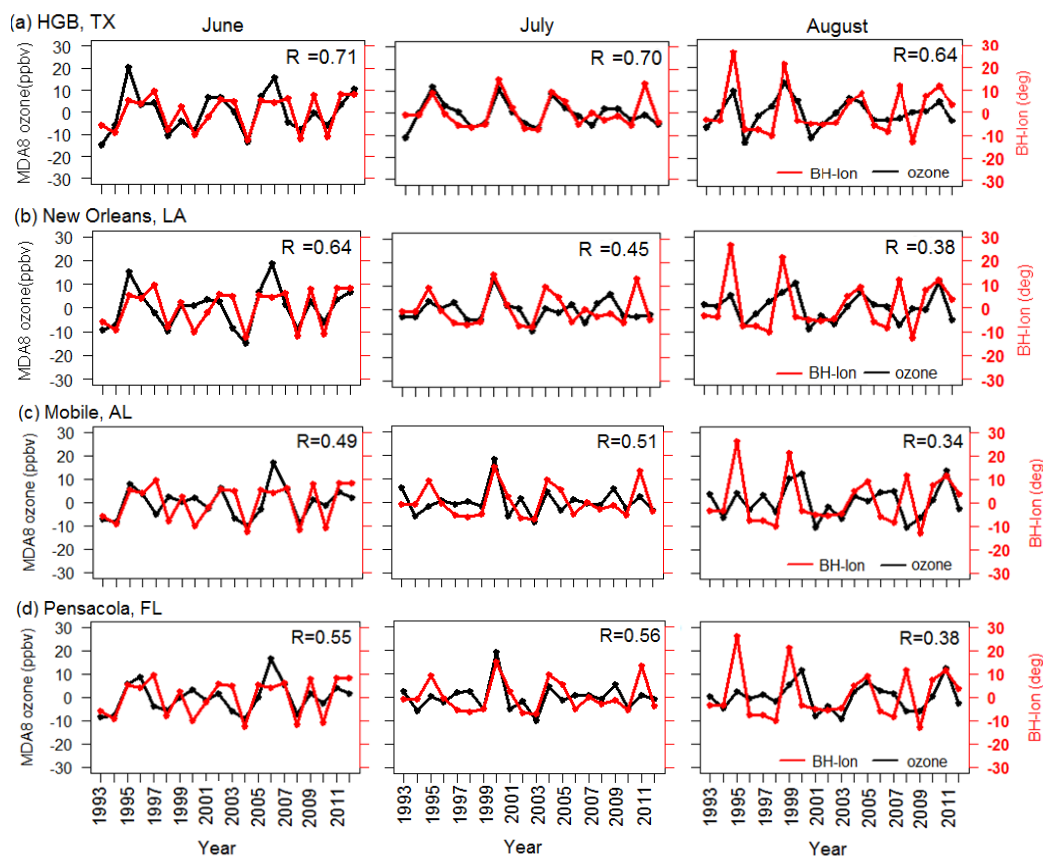
636 at one or more monitors in HGB is higher than 75 ppbv.

637

638

639

640



641 Figure 6. The time series of detrended BH-Lon (red line) and MDA8 ozone (black line)  
642 during June, July and August over the HGB region, TX (a), New Orleans, LA (b),  
643 Mobile, AL (c) and Pensacola, FL (d). The correlation coefficients between BH-Lon  
644 and ozone are shown in each figure.

645

646

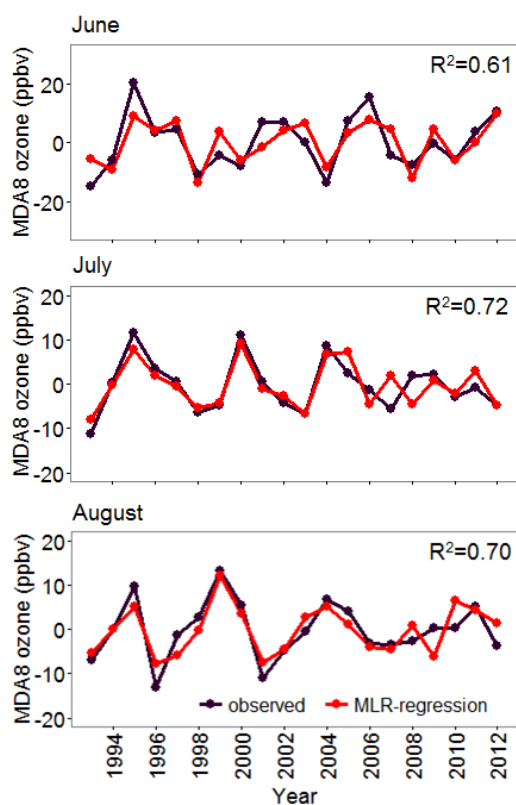
647

648

649



650



651

652 Figure 7. Time series of observed HGB-mean MDA8 ozone (black line) and

653 MLR-regressed ozone (red line) in June (top), July (middle) and August (bottom). The

654 data presented are detrended.

655

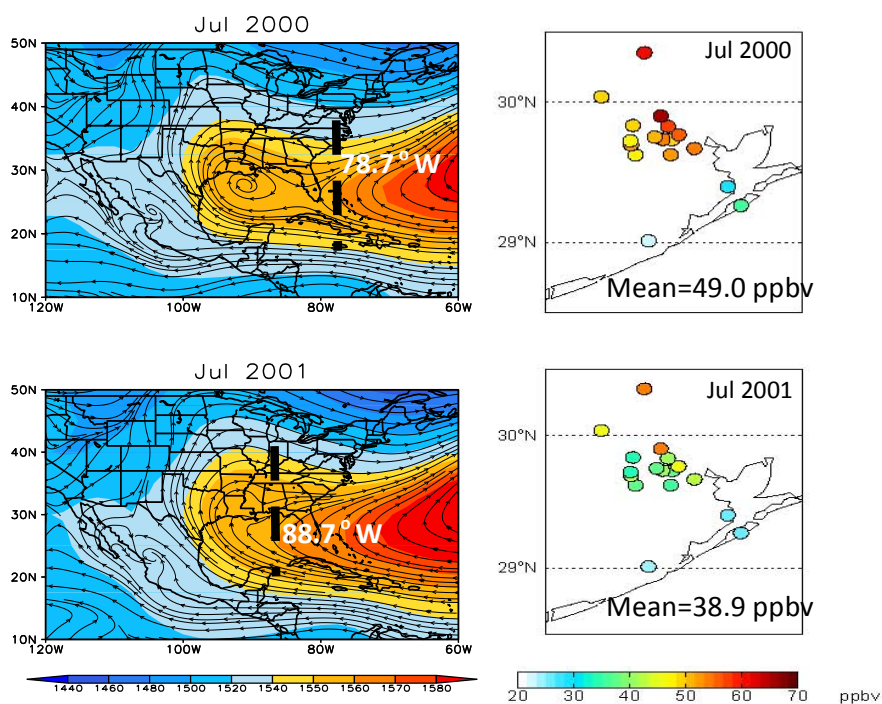
656

657

658

659

660



661

662 Figure 8. (Left) 850 hPa geopotential height (gpm) and stream line for the month f

663 July 2000 and July 2001. The black dashed line shows the longitude of the BH-Lon

664 (values shown in white). (Right) MDA8 ozone concentrations at the CAMS sites in

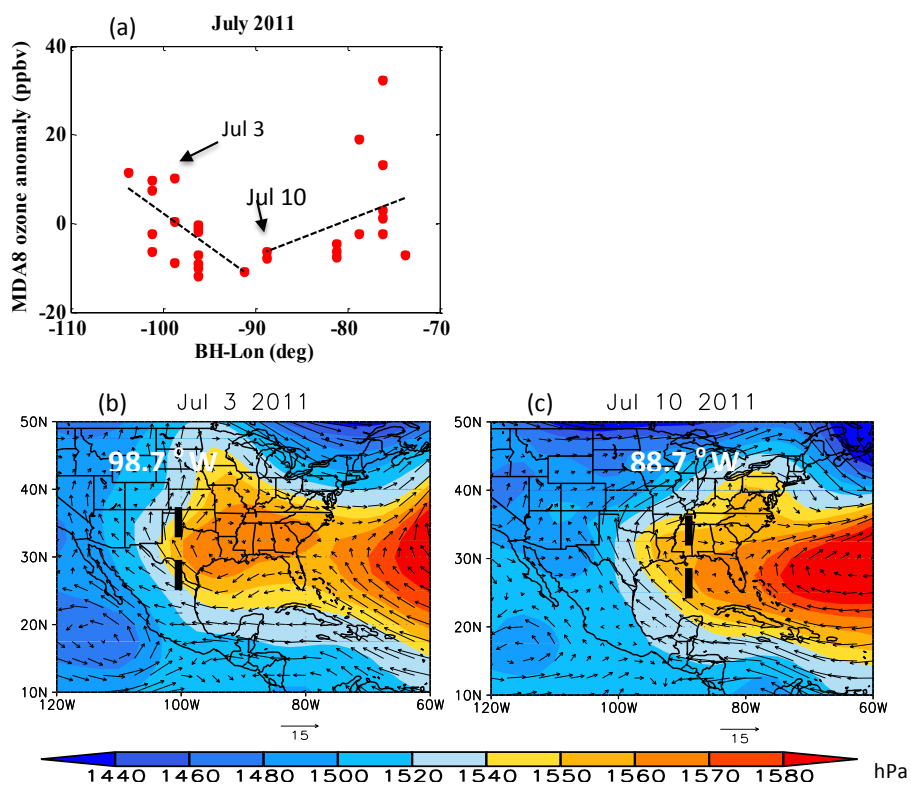
665 HGB for July 2000 and July 2001.

666

667

668

669



670

671 Figure 9. (a) Relationship between daily ozone anomaly (y-axis) and daily BH-Lon

672 (y-axis) for July 2011. (b-c) Distribution of SLP (color contours) and 850hPa wind

673 fields (arrows) on July 3rd (b) and July 10th 2011 (c). The black dashed line shows the

674 longitude of the BH-Lon (values shown in white).

675

676

677

678